MIT Libraries | DSpace@MIT

MIT Open Access Articles

Adult bone marrow stromal cell-based tissue-engineered aggrecan exhibits ultrastructure and nanomechanical properties superior to native cartilage

The MIT Faculty has made this article openly available. ***Please share*** how this access benefits you. Your story matters.

Citation: Lee, H.-Y. et al. "Adult bone marrow stromal cell-based tissue-engineered aggrecan exhibits ultrastructure and nanomechanical properties superior to native cartilage." Osteoarthritis and Cartilage 18 (2010): 1477-1486.

As Published: http://dx.doi.org/10.1016/j.joca.2010.07.015

Publisher: Elsevier Ltd.

Persistent URL: http://hdl.handle.net/1721.1/67287

Version: Author's final manuscript: final author's manuscript post peer review, without publisher's formatting or copy editing

Terms of use: Creative Commons Attribution-Noncommercial-Share Alike 3.0

Massachusetts Institute of Technology

NIH Public Access
Author Manuscript
Osteoarthritis Cartilage. Author manuscript; available in PMC 2011 November 1.

Published in final edited form as:
Osteoarthritis Cartilage. 2010 November ; 18(11): 1477–1486. doi:10.1016/j.joca.2010.07.015.

Adult Bone Marrow Stromal Cell-Based Tissue-Engineered Aggrecan Exhibits Ultrastructure and Nanomechanical Properties Superior to Native Cartilage

H.-Y. Lee, S.M.[a], **P. W. Kopesky, Ph.D.**[b], **A. Plaas, Ph.D.**[c], **J. Sandy, Ph.D.**[c], **J. Kisiday, Ph.D.**[d], **D. Frisbie, Ph.D.**[d], **A. J. Grodzinsky, Ph.D.**[a,b,e], and **C. Ortiz, Ph.D.**[f,*]

[a]Department of Electrical Engineering and Computer Science, Massachusetts Institute of Technology, Cambridge, MA

[b]Department of Biological Engineering, Massachusetts Institute of Technology, Cambridge, MA

[c]Department of Biochemistry, Rush University Medical Center, Chicago, IL

[d]Equine Orthopaedic Research Center, Colorado State University, Fort Collins, CO

[e]Department of Mechanical Engineering, Massachusetts Institute of Technology, Cambridge, MA

[f]Department of Materials Science and Engineering, Massachusetts Institute of Technology, Cambridge, MA

Summary

Objective—To quantify the structural characteristics and nanomechanical properties of aggrecan produced by adult bone marrow stromal cells (BMSCs) in peptide hydrogel scaffolds and compare to aggrecan from adult articular cartilage.

Design—Adult equine BMSCs were encapsulated in 3D-peptide hydrogels and cultured for 21 days with TGF-β1 to induce chondrogenic differentiation. BMSC-aggrecan was extracted and compared with aggrecan from age-matched adult equine articular cartilage. Single molecules of aggrecan were visualized by atomic force microcopy-based imaging and aggrecan nanomechanical stiffness was quantified by high resolution force microscopy. Population-averaged measures of aggrecan hydrodynamic size, core protein structures and CS sulfation compositions were determined by size-exclusion chromatography, Western analysis, and fluorescence-assisted carbohydrate electrophoresis (FACE).

Results—BMSC-aggrecan was primarily full-length while cartilage-aggrecan had many fragments. Single molecule measurements showed that core protein and GAG chains of BMSC-aggrecan were markedly longer than those of cartilage-aggrecan. Comparing full-length aggrecan of both species, BMSC-aggrecan had longer GAG chains, while the core protein trace lengths were similar. FACE

*Corresponding author. Tel.: +1 617 452 3084, cortiz@mit.edu.

Contributions: H.-Y. Lee and P. W. Kopesky: (1) design of study, acquisition of data, and analysis and interpretation of data, (2) drafting and revising the article for important intellectual content, and (3) final approval of the submitted article.
A. Plaas, J. D. Sandy, J. Kisiday, D. Frisbie, A. J. Grodzinsky, C. Ortiz (cortiz@mit.edu): (1) design of study and interpretation of data, (2) revising the article for important intellectual content, and (3) final approval of the submitted article.

Competing interest statement: All the authors have no financial and personal relation ships with other people or organizations that could potentially and inappropriately influence their work and conclusions.

Publisher's Disclaimer: This is a PDF file of an unedited manuscript that has been accepted for publication. As a service to our customers we are providing this early version of the manuscript. The manuscript will undergo copyediting, typesetting, and review of the resulting proof before it is published in its final citable form. Please note that during the production process errors may be discovered which could affect the content, and all legal disclaimers that apply to the journal pertain.

NIH-PA Author Manuscript
NIH-PA Author Manuscript
NIH-PA Author Manuscript

NIH-PA Author Manuscript

NIH-PA Author Manuscript

NIH-PA Author Manuscript

analysis detected a ~1:1 ratio of chondroitin-4-sulfate to chondroitin-6-sulfate in BMSC-GAG, a phenotype consistent with aggrecan from skeletally-immature cartilage. The nanomechanical stiffness of BMSC-aggrecan was demonstrably greater than that of cartilage-aggrecan at the same total sGAG (fixed charge) density.

Conclusions—The higher proportion of full-length monomers, longer GAG chains and greater stiffness of the BMSC-aggrecan makes it biomechanically superior to adult cartilage-aggrecan. Aggrecan stiffness was not solely dependent on fixed charge density, but also on GAG molecular ultrastructure. These results support the use of adult BMSCs for cell-based cartilage repair.

Keywords

Aggrecan; Bone-marrow stromal cell; Cartilage repair; Tissue engineering; Self-assembling peptide; Molecular Nanomechanical properties

Introduction

Tissue engineering substitutes have great potential for the restoration of the biological function of damaged and diseased cartilage,[1] which has limited intrinsic self-regeneration capabilities. Approaches to cartilage tissue engineering involve numerous design considerations involving cell source (e.g. chondrocytes, synoviocytes, marrow/adipose-derived progenitor cells), biocompatible scaffold chemistry and morphology, bioactive signaling factors that promote cellular differentiation, maturation, and extracellular matrix synthesis, mechanical stimulation, gene therapy, microenvironmental factors and bioreactors.[2] While many tissue engineering methodologies produce cartilage-like neo-tissues with similar macromolecular components compared to the native cartilage extracellular matrix (ECM), a major challenge is to produce constructs having biochemical, structural and biomechanical properties that are *functionally* equivalent to cartilage *in vivo*.[3]

The overall composition and organization of neocartilage is typically characterized via biochemical[4,5], histological and immunohistochemical[6] measures, while ECM molecular constituents have been analyzed using various chromatographic[7] and electrophoretic techniques[8,9]. Tissue-level biomechanical measurements to quantify the compressive, tensile and shear behavior[10,11] of neocartilage are related to and ultimately determined by the macromolecular constituents and assembly of the ECM[12,13]. Recently, high resolution imaging and nanomechanical methodologies have been developed to directly visualize the detailed *intra*molecular structure and probe the nanoscale mechanical properties of various ECM constituents (e.g., aggrecan[14,15], collagen[16,17], hyaluronan[18]). These techniques provide an understanding of molecule-to-molecule variability, intramolecular and local nanoscale properties, and the ability to assess properties of selected sub-populations that cannot be revealed by macroscopic measures which provide population averages. The combination of new nanotechnological approaches with traditional biochemical, histological, and macroscopic mechanical methods, can greatly assist in understanding, evaluating and optimizing a proposed tissue engineered strategy.

Because aggrecan is the dominant compressive load-bearing macromolecule in cartilage ECM[19], its expression, synthesis, organization, and turnover are often used as biomarkers of the chondrogenic potential of bone marrow stromal cells (BMSCs) in cell-based cartilage tissue engineering[20-22]. Recent studies showed that the sulfated glycosaminoglycan (sGAG) content of BMSC-seeded agarose and self-assembling peptide hydrogels was lower than that in parallel hydrogels seeded with chondrocytes from skeletally-immature cartilage[20,23], and varied with scaffold material[23,24]. Aggrecan accumulated within BMSC-seeded constructs was structurally different from that in native cartilage or in similar hydrogels seeded with

NIH-PA Author Manuscript

NIH-PA Author Manuscript

NIH-PA Author Manuscript

chondrocytes. In agarose, BMSC-synthesized aggrecan was shown by Western analysis to be primarily full-length[22]; in the peptide gel, atomic force microscopy (AFM) imaging showed that BMSC-aggrecan had longer core protein and larger GAG chain length[23]. The chondrogenic potential of adult human BMSCs was found to be independent of age or osteoarthritis (OA)[25], an advantage of using BMSCs over chondrocytes for autologous cell-based cartilage repair[26] for older OA patients, where the source and capacity of chondrocytes are limited. Given these advantages of BMSC-based cartilage repair, rigorous molecular-level characterization of BMSC-produced ECM is needed to further understand adult BMSC chondrogenesis.

The goal of this study was to investigate aggrecan produced by adult equine BMSCs encapsulated in peptide hydrogels and induced to undergo chondrogenic differentiation and to compare with aggrecan extracted from age-matched adult equine articular cartilage. The detailed molecular structure and properties of aggrecan were quantitatively assessed using high resolution AFM-based approaches. First, the ultrastructure of these two aggrecan populations was investigated via AFM-based single molecule imaging. Secondly, the aggrecan-GAG sulfation patterns and extent of core protein proteolysis was characterized using fluorescence-assisted carbohydrate electrophoresis (FACE)[8], Western blot, and size-exclusion chromatography analyses. Finally the nanomechanical properties of these two aggrecan populations were evaluated using high resolution force microscopy. Adult BMSC-peptide aggrecan demonstrated ultrastructural features and GAG sulfation similar to those of skeletally-immature (young) cartilage aggrecan, and had increased compressive stiffness compared to adult cartilage aggrecan.

Methods

Tissue Harvest

Cartilage tissue was harvested aseptically from the femoropatellar groove, and bone marrow was harvested from three skeletally-mature (2-5 year-old adults) mixed-breed horses as described previously[23]. Horses were euthanized at Colorado State University for reasons unrelated to this study, and for conditions that would not affect either cartilage or bone marrow.

Marrow Stromal Cell Isolation

BMSCs were isolated and stored as previously described[23]. Marrow samples were washed in PBS and fractionated by centrifugation to separate the nucleated cells from the red blood cells. BMSCs were isolated by differential adhesion to tissue culture plastic. After BMSC colonies reached local confluence, cells were detached and reseeded at 6×10^3 cells/cm^2, expanded to ~3×10^4 cells/cm^2 over three days, and cryo-preserved. Before hydrogel encapsulation, BMSCs were thawed and plated at 6×10^3 cells/cm^2. After 3 days, cells were detached (passage-1) and reseeded at 6×10^3 cells/cm^2, and expanded for three days prior to encapsulation in peptide hydrogels.

Hydrogel Encapsulation and Culture

KLD12 peptide with the sequence AcN-$(KLDL)_3$-CNH_2 was synthesized by the MIT Biopolymers Laboratory (Cambridge, MA) using an ABI Model 433A peptide synthesizer with FMOC protection. BMSCs were encapsulated in 0.35% (w/v) KLD12 peptide at a concentration of 10×10^6 cells/ml using acellular agarose casting molds to initiate peptide assembly as described previously[23]. BMSC-seeded disks (6.35mm-diam×1.6mm-thick) were cultured in high glucose DMEM (Invitrogen, Carlsbad, CA) supplemented with 1% ITS+1 (final concentration: 10μg/ml insulin, 5.5μg/ml transferrin, 5ng/ml sodium selenite, 0.5mg/ml bovine serum albumin, 4.7μg/ml linoleic acid, Sigma-Aldrich), 0.1μM dexamethasone (Sigma-Aldrich, St. Louis, MO), 37.5μg/ml ascorbate-2-phosphate (Wako Chemicals, Richmond,

NIH-PA Author Manuscript

NIH-PA Author Manuscript

NIH-PA Author Manuscript

VA), 1% PSA, 10mM HEPES, 400μM L-proline, 1mM sodium pyruvate, and 1% NEAA, with 10ng/ml rhTGF-β1 (R&D Systems, Minneapolis, MN) with medium changes every 2-3 days. Disks were cultured for 21 days.

Aggrecan Extraction

Aggrecan was extracted from BMSC-peptide gels and native articular cartilage (Fig. 1a) with 4M guanidine HCl, 100mM sodium acetate, pH 6.8, containing Protease Complete inhibitor mix (Roche, Indianapolis, IN) for 48 hours at 4°C with agitation[27]. Extracts were adjusted to 1.58g/ml by the addition of CsCl and centrifugation at 470,000 g_{av} for 72 hours at 4°C. The D1 fractions (>1.54g/ml) were desalted by dialysis against water, dried and used for AFM imaging, nanomechanical testing, and Western analysis. Unfractionated GuHCl extracts were also desalted and used for FACE analysis[8].

AFM Imaging

D1 aggrecan samples at 50μg sGAG/ml in MilliQ water were deposited on 3-aminopropyltriethoxysilane (APTES; Sigma Aldrich, St. Louis, MO) functionalized muscovite mica substrates (SPI Supplies, West Chester, PA) and rinsed with MilliQ water after 30 minutes, as previously described[14]. Electrostatic interactions between the positively charged APTES-mica and the negatively charged GAG chains retained aggrecan on the surface in a relatively flat conformation[14], despite rinsing in water. Tapping mode imaging (Fig.1b) was performed in ambient conditions with a Nanoscope IIIa Multimode AFM (Veeco Instruments, Plainview, NY) and Super Sharp Silicon AFM probes (nominal cantilever spring constant=42N/m, nominal tip end radius <5 nm; Nanosensors, Switzerland). A thin layer (0.2-1nm) of absorbed water is present on mica under ambient conditions[28] which partially hydrates the aggrecan.

Quantification of Aggrecan Single Molecule Dimensions

AFM height images were digitized into pixels and aggrecan structural features (ie. core protein and GAG trace length) were traced and calculated automatically with a custom Matlab program (The MathWorks, Natick, MA) or manually with SigmaScan Pro image analysis software (SPSS Science, Chicago, IL). Full-length aggrecan were identified quantitatively by the presence of G1 and G3 domains having increased height (>0.5nm) at the ends of the core protein.

Aggrecan Nanomechanical Testing

Microcontact printing[29] was employed to produce micrometer-sized hexagonally-patterned surfaces of densely packed, chemically end-grafted aggrecan surrounded by a neutral hydroxyl-terminated self-assembled monolayer (11-mercaptoundecanol, $HS(CH_2)_{11}OH$, OH-SAM)[15] (Fig. 1c). A Multimode picoforce Nanoscope IV AFM (Veeco Instruments, Plainview, NY) was used to perform compressive nanomechanical testing with an OH-functionalized spherical colloidal probe tip[15] (cantilever spring constant ~0.12N/m, tip end radius ~2.5μm; Novascan, Ames, IA). Two measurements were employed to assess the mechanical stiffness of the aggrecan. First, the absolute compressed height *H* of aggrecan as a function of applied normal force was obtained by scanning parallel to the substrate surface and across the hexagon region[15] (Fig. 1d) using contact mode imaging over a wide range of normal forces (0~30 nN), and in aqueous solutions of 0.001 to 1M NaCl (pH~5.6). Secondly, normal compression of aggrecan was performed by having the probe tip approach perpendicularly to the substrate (z-piezo displacement velocity =2μm/s, Fig. 1e). Raw data were converted to normal force as a function of tip-to-substrate distance, *D* as described previously[15]. D_o is defined as the *D* where the force first increases above noise level. Normal stress was calculated from the normal force using the surface element integration method[15,30]. The total sGAG content within a hexagon

NIH-PA Author Manuscript

NIH-PA Author Manuscript

NIH-PA Author Manuscript

on the gold substrate was measured by dimethylmethylene blue dye assay (DMMB)[4] after testing. The initial sGAG density prior to compression, calculated by dividing the sGAG content by pattern volume, was ~20mg/ml (one aggrecan molecule per ~25nm×25nm) at 0.1M NaCl for both BMSC-peptide and cartilage-extracted aggrecan samples. sGAG density during compression was calculated as a function of compressed height by normalizing the total sGAG content under the probe tip to the reduced compressed volume. (This estimate of density assumes minimal outward "bulging" of aggrecan at the radial periphery of the layer under the tip. Since the tip diameter (2R)$\gg D_o$ and, given the lateral constraint of the adjacent uncompressed aggrecan, this assumption is reasonably well justified.)

Core Protein Heterogeneity

Aggrecan core protein heterogeneity was analyzed by Western blotting. Samples were treated with protease-free chondroitinase ABC (30mU/100μg GAG), keratanase II (0.5mU/100μg GAG) and endo-β-galactosidase (0.5mU/100μg GAG) (Seikagaku, Tokyo, Japan) and digests corresponding to 10μg GAG were loaded on 4-15% polyacrylamide gels and probed with antibodies to the aggrecan G1 (JSCATEG)[31].

Relative Hydrodynamic Sizes of Aggrecan and GAG

Sephacryl S-1000 and Superose 6 FPLC chromatography (GE Healthcare, Piscataway, NJ) were used to characterize the hydrodynamic size distributions of aggrecan monomers and their constituent GAG chains, respectively. Aggrecan (200μg sGAG) was eluted on S-1000 at 30 ml/hr with 0.5M sodium acetate at pH 6.8. For GAG analysis, 100μg aggrecan was digested with 50μg proteinase K in 200μl ammonium acetate (pH 7.2) for 48 hrs at 60 °C and 100μl of the digest was eluted on Superose 6. Fractions (0.5 ml) were collected at 0.5ml/min and assayed for sGAG by DMMB. The void volume V_o and total volume V_t were determined using 0.5μm polystyrene beads and phenol red, respectively. The partition coefficient (K_{av}) was estimated as $(V_e - V_o)/(V_t - V_o)$, for each eluted fraction V_e.

FACE Analysis of GAG Sulfation

FACE analysis was performed on proteinase K digests of BMSC-peptide aggrecan from 3 different adult horses and cartilage-extracted aggrecan from 1 adult horse. Samples containing 2-10μg of sGAG were digested with chondroitinase ABC, disaccharide products fluorotagged by reductive amination with 2-aminoacrodone, prior to separation and quantitation by FACE[8].

Statistical Analyses

Aggrecan and GAG molecular dimensions are reported as mean±SD in text and in figures for population distribution. For data-sets having a unimodal distribution, a Gaussian fit was used to test for normality, and the goodness of fit was evaluated by R^2 (the summed mean squares of the regression divided by the summed mean squares of the data). For normally distributed data-sets, two-tailed, unpaired Student t-tests were performed to test for differences of the means, with significance set at $p<0.05$. For non-unimodal distributions, a two-sample Kolmogorov-Smirnov (K-S) test was performed to compare distributions of molecular dimensions. For comparison between groups, 95% confidence intervals were used.

Results

Single molecule ultrastructure of BMSC-peptide and native cartilage aggrecan

AFM height images compare the ultrastructure of BMSC-peptide aggrecan (Fig. 2a-c) to cartilage-extracted aggrecan (Fig. 2d-f). Individual aggrecan molecules were directly visualized and the details of their intramolecular structure including the core protein and

NIH-PA Author Manuscript

NIH-PA Author Manuscript

NIH-PA Author Manuscript

constituent GAG chains identified (Fig. 2b,c,e,f). In many cases, the brighter globular domains (G1, G3) at the ends of the core protein (arrows in Fig. 2a,d) could be identified by their increased height (>0.5 nm) relative to the rest of the molecule. Aggrecan with globular domains at both N (G1)- and C (G3) termini were identified as "full-length," i.e., those which had not been enzymatically cleaved along the core protein[32,33]. The molecular dimensions of the aggrecan from the two sources were strikingly different. The BMSC-peptide aggrecan had noticeably longer GAG chains than cartilage-extracted aggrecan (Fig.2b,c vs. Fig. 2e,f, quantified below). Moreover, short fragments (Fig. 2d, asterisks) were more pronounced in the cartilage-extracted aggrecan population than in BMSC-peptide aggrecan (quantified below).

Core protein length distribution and heterogeneity

The distributions of the core protein trace length for the BMSC-peptide and cartilage-extracted aggrecan were markedly different (K-S test, $p<0.0001$, Fig. 3a,b), with BMSC-peptide aggrecan =440±138nm (mean±SD) and cartilage-extracted aggrecan =220±142nm. While the length distributions were broad and nearly bimodal (Fig. 3a,b), the constituent sub-populations of *full-length* aggrecan (Fig.2c,d) were both normally distributed with peaks at 487nm and 475nm that were not significantly different from each other ($p=0.32$). A large proportion (~40%) of the BMSC-peptide aggrecan was full-length (Fig. 3a,c), whereas the majority of the cartilage aggrecan (~86%) were fragments (Fig. 3b,d) consistent with proteolytic degradation. Full-length cartilage-extracted aggrecan comprised a smaller sample size ($n=20$, Fig. 3d) due to the lower proportion of full-length aggrecan observed in the whole population. The difference in size of the molecular populations was also seen in the S-1000 chromatograms (Fig. 3e): BMSC-peptide aggrecan eluted earlier ($K_{av}=0.25$) than the cartilage-extracted aggrecan ($K_{av}=0.42$), consistent with the larger average hydrodynamic size of BMSC-peptide aggrecan.

Western analyses were performed on the same samples to further assess the heterogeneity of the core protein constituents by using antibodies against the G1 domain of the core proteins. The BMSC-peptide aggrecan showed a greater abundance of high-molecular-weight species reacting with anti-G1 antibody, consistent with a larger population of full-length aggrecan (Fig. 3f). The major G1-immunoreactive fragment seen in both the BMSC-peptide and cartilage-extracted aggrecan samples was similar to the molecular weight of a previously characterized calpain[33]-generated "double-globe" species (~120kDa). In addition, the G1-containing bands between 56-101kDa suggest that cartilage aggrecan may have undergone more extensive proteolysis than the BMSC aggrecan. However, it may be difficult to assess the total extent of proteolysis from this technique as such fragments could remain in lower density fractions and be less well recovered.

GAG Chain Length and Sulfation

The distribution of individual GAG chain lengths within a single representative full-length aggrecan in the BMSC and cartilage populations of Fig. 3c,d is shown in Fig. 4a,b, respectively. The selected full-length BMSC-peptide aggrecan has longer average GAG length (47±8nm, $n=41$ chains, Fig. 4a) than that of the single cartilage-aggrecan (17±7nm, $n=44$ chains, Fig. 4b). The GAG chains of this BMSC-peptide aggrecan also have a broader length distribution than that of the cartilage-extracted aggrecan (Fig. 4a,b). For multiple aggrecan molecules, GAG chain lengths were measured and an average chain length per molecule was calculated (Figs. 4c,d). The mean of the average GAG length per molecule was 44±10nm for BMSC-aggrecan ($n=299$, Fig. 4c) and 20±4nm for cartilage-aggrecan ($n=87$, Fig. 4d). The n (number of measured aggrecan molecules) in Fig. 4d was smaller than that in Fig. 3b because some fragments did not have detectable GAG chains. For the full-length aggrecan populations of Fig. 3c,d, the corresponding GAG trace length of BMSC-peptide aggrecan was about twice as long as that of cartilage-aggrecan (Fig 4e,f). For both "all observed" (Fig. 4c,d) and "full-

NIH-PA Author Manuscript

NIH-PA Author Manuscript

NIH-PA Author Manuscript

length" (Fig. 4e,f) aggrecan populations, the mean GAG chain length per aggrecan molecule of the BMSC-peptide aggrecan was significantly longer than that of cartilage-extracted aggrecan ($p<0.0001$). For each population (BMSC-peptide or cartilage-extract), the "all observed" and "full-length" aggrecans had similar GAG lengths ($p=0.175$ and 0.642, respectively).

The relative hydrodynamic size of BMSC- and cartilage-aggrecan GAG chains was also assessed by Superose 6 size-exclusion chromatography (Fig. 3g). The BMSC-aggrecan GAGs eluted at K_{av} =0.50 while cartilage-extracted GAGs eluted at K_{av} =0.71, corresponding to average chain lengths of ~60 disaccharides (27kDa, corresponding to ~60nm contour length) and ~30 disaccharides (13kDa, ~30nm), respectively[35], assuming the proteinase K used here and the papain digestion used previously[35] generated single CS chains.

FACE analyses showed that aggrecan CS chains produced by peptide-encapsulated BMSCs from 3 adult equines were composed of approximately equimolar amounts of 4- and 6-sulfated disaccharides, a ratio characteristic of skeletally-immature and growing cartilage. In contrast, the adult cartilage-extracted aggrecan showed a higher proportion of 6-sulfated disaccharides, typical of adult cartilage[36].

Aggrecan Compressive Stiffness

The three-dimensional AFM height images of microcontact printed substrates verified the presence of clear hexagonal patterns of both BMSC-peptide and cartilage-extracted aggrecan (Fig. 5a,b). Consistent with previous results[15], the aggrecan height, *H*, decreased monotonically with increasing ionic strength and with increasing normal force during a lateral scan and reached the final incompressible height by ~30nN force (Fig. 5c,d). The initial heights at low force reflect the relative differences in lengths of the two aggrecan populations observed via AFM imaging. At any given ionic strength, the BMSC-peptide aggrecan pattern showed ~2-3 fold longer initial height than cartilage-aggrecan.

In the one-dimensional force-distance measurements (Fig. 5e,f), normal force increased markedly with compression (decreasing *D*) as observed previously with fetal bovine aggrecan[15]. At any given ionic strength, the BMSC-peptide aggrecan exerted a repulsive force against tip at longer D_o (e.g., D_o ~600nm for BMSC-peptide aggrecan and ~200nm for cartilage-aggrecan in 0.001M NaCl (Fig 5e,f)), reflecting the larger initial height and stronger electrostatic repulsion interactions of BMSC-peptide aggrecan. The compressive properties studied with these two different nanomechanical methodologies, height-force and force-distance, coincide well with each other (Fig. 5g). The small difference between *H* and *D* at low force (<5nN) was likely due to the tare force (~100pN) necessary to enable stable feedback during imaging[15].

Finally, to directly compare the compressive stiffness of the two aggrecan populations independent of their different initial heights (i.e., core protein lengths), the force-distance curves of Fig. 5e,f were converted to stress versus DMMD-measured sGAG-concentration (see Methods). At physiological ionic strength (0.1M NaCl), the normal stress increased markedly with increasing compression (i.e., density of compressed GAG), but much more dramatically for the BMSC-peptide aggrecan (Fig. 6).

Discussion

This study of aggrecan macromolecules from tissue-engineered constructs and native cartilage involved the combination of high resolution AFM-based techniques to quantify nanoscale structure and nanomechanical properties. Such an approach can provide a platform for optimization of cell source, scaffold and culture conditions. AFM imaging enabled

NIH-PA Author Manuscript

NIH-PA Author Manuscript

NIH-PA Author Manuscript

visualization of single molecules and their inter- and intramolecular heterogeneity. Marked differences were observed between adult BMSC- and cartilage-aggrecan populations. BMSC-aggrecan was predominantly full-length with fewer proteolytically degraded fragments and much longer CS-GAG chains than cartilage aggrecan. These detailed AFM-based measurements were consistent with size-exclusion chromatography and Western analyses. In addition, AFM nanomechanical measurements showed that the compressive stiffness of the BMSC-aggrecan was markedly higher than that of cartilage aggrecan. Taken together, these results suggest that adult BMSC-aggrecan exhibits characteristics more similar to those of skeletally-immature growth cartilage than to adult cartilage.

Imaging of single molecules revealed that aggrecan synthesized by adult BMSCs in peptide hydrogel had an overall morphology qualitatively similar to that in adult cartilage, consisting of a GAG-functionalized core protein[19]. However, the two aggrecan populations had strikingly different molecular dimensions (Figs. 2›3). Based on AFM imaging, 50% of the BMSC-aggrecan had a core protein length >400 nm, compared to only 16% of the cartilage-aggrecan (Fig. 3a,b). S-1000 chromatography demonstrated average molecular sizes that were consistent with AFM-based results. Western analyses suggested that the major G1-immunoreactive constituents of cartilage-aggrecan were fragments which have been previously shown to be generated by aggrecanases[32] (G1-NITEGE) and m-calpain[33] (G1-G2-GVA), though the action of other proteinases cannot be excluded. In contrast, BMSC-peptide aggrecan was predominantly full-length, typical of aggrecan from immature cartilage[14,37]. The activity of aggrecan proteolytic enzymes is known to be regulated by TGF-β, but evidence exists for both inhibition[38] and upregulation[39] of proteolysis. Interestingly, if compared to the aggrecan produced by *adult articular chondrocytes* under the identical conditions with TGF-β stimulation[23], the adult BMSC-aggrecan have a larger proportion of full-length core proteins than the adult chondrocyte-aggrecan. The full-length BMSC- and cartilage-aggrecan had similar core protein trace lengths exhibiting a Gaussian distribution (Fig. 3c,d). Together, these results suggest that the decreased average core protein trace length seen in the entire cartilage-aggrecan population was due to proteolytic degradation.

The GAG chains of BMSC-aggrecan were found to be more than two times longer than that of cartilage-aggrecan (Fig. 4). CS chain length has been shown to decrease with age in cartilage tissue[27,40] and is also smaller when synthesized by adult chondrocytes cultured *in vitro*, reflecting an age dependent alteration of aggrecan-GAG synthesis[41]. Longer GAGs are prevalent in aggrecan from immature cartilage[40,42], growth plate[35] and newly synthesized aggrecan after injury[43], as well as during the early stages of osteoarthritis[44]. The latter two studies hypothesized that the increased CS chain length in injured and OA-cartilage were indicative of growth cartilage metabolic phenotype. The CS sulfation fine structure analyses are also consistent with such a conclusion. The sulfation patterns of CS-GAGs analyzed by FACE have been studied previously as a characteristic of animal age, GAG chain termination, tissue differentiation and development[42,45,46]. Adult BMSCs synthesized CS with ~1:1 ΔDi6S-to-ΔDi4S ratio, similar to that observed previously in skeletally-immature and growing cartilage[35,36], while adult cartilage contained aggrecan predominantly with 6S-sulfated CS (Fig. 4h), consistent with previous studies[36]. The differences in the GAG structure between the two aggrecan populations in this study suggest that adult BMSCs undergoing chondrogenesis in peptide hydrogels exhibit a very different pattern of glycosylation than adult chondrocytes in native tissue.

The exact mechanisms whereby cells control CS chain length and sulfation pattern are still under study. TGF-β has been shown to affect CS-GAG synthesis; for example, TGF-β-stimulated fibroblasts produced elongated CS-GAG chains. In our recent study[23] in which animal-matched articular chondrocytes and BMSCs from immature or adult equines were cultured under identical conditions for 3 weeks in the same peptide hydrogel and in the same

NIH-PA Author Manuscript

NIH-PA Author Manuscript

NIH-PA Author Manuscript

(TGF-β1-containing) medium, the BMSCs produced longer GAG chains than the animal-matched chondrocytes. This observation suggests that longer GAG chains are not just a result of TGF-β stimulation, but also a reflection of cell type. Since the GAGs contribute to the stiffness of cartilage, and proteolytic loss of protein-bound GAGs is a major characteristic of osteoarthritis, the BMSC-aggrecan would appear to have a more favorable GAG structure for cartilage mechanical function than the adult cartilage-aggrecan.

A major finding in the present study was the demonstration that BMSC-aggrecan was demonstrably stiffer in nanomechanical compression than cartilage-aggrecan. The BMSC-aggrecan population had a larger average core protein length; thus, its pattern height (Fig. 5c,d) and tip-substrate separation distance were larger than that of cartilage-aggrecan at the same normal force and ionic strength (Fig. 5e,h). In order to compare their intrinsic stiffness independent of aggrecan dimensions, the force-distance curves were converted to curves of stress versus DMMB-measured sGAG concentration (Fig. 6). Upon compression by the AFM tip, which increased sGAG concentration under the tip, the BMSC-aggrecan exhibited larger compressive stress. The macroscopic compressive moduli of bulk cartilage are known to correlate well with the concentration of specific ECM constituents[12,47] such as collagen and GAG; and the correlation with GAG is ascribed to sGAG fixed charge density[47]. However, our observation indicates that at the nanoscale, not only the constituent sGAG *charge* density, but the molecular structure and dimensions of the GAGs can affect compressive stiffness. The longer CS chains of BMSC-aggrecan may result in more intermolecular entanglement, steric and stronger excluded volume effects during deformation. In addition, electrostatic interactions between highly charged, closely-spaced rod-like chains are known to cause higher and more nonlinear increases in repulsive stress compared to that caused by compression of spatially homogeneous densities of fixed charge[15,48]. These phenomena may be particularly important in localized regions such as the microenvironment of cells, e.g. the pericellular matrix, which can be stimulated by mechanical forces. It also suggested that the stiffer BMSC-produced constructs in comparison with the chondrocyte-produced constructs we reported previously[23] may not only due to the more total matrix content of the BMSC construct, but also due to the longer GAG chain and core protein length of BMSC-aggrecan. The greater stiffness of BMSC-aggrecan is also an attribute of immature native aggrecan[49] and may be advantageous to cartilage repair.

Taken together, the nanomechanical properties of adult BMSC-peptide aggrecan appear superior to that of adult native cartilage aggrecan. Adult BMSCs are thus a promising cell candidate for cell-based tissue engineering for cartilage repair and regeneration. Of course, additional challenges must be met to achieve successful cartilage repair *in vivo*, including the assembly of an appropriate collagen architecture and the synthesis and assembly of other matrix macromolecules to enable integration with the surrounding tissues. The combined methodologies utilized here can be applied to optimize the cell source and culture for engineering desired ECM assemblies. The detailed structure and nanomechanical properties of aggrecan and other ECM molecules can provide insights into the molecular determinants to the integrity and functionality of cartilage repair.

Acknowledgments

The authors thank Sunita Darbe for contributions to chromatography analyses.

Role of the funding source: This work was funded by NIH grants EB003805 and AR33236, NSF grants NIRT-0403903 and CMMI-0758651), NIH Molecular, Cell, and Tissue Biomechanics Training Grant (PWK), and Whitaker Health Science Fund Fellowship. The sponsors had no role in the design, analysis and writing of the manuscript.

NIH-PA Author Manuscript

NIH-PA Author Manuscript

NIH-PA Author Manuscript

References

1. Langer RS, Vacanti JP. Tissue engineering: The challenges ahead. Scientific American 1999;280(4): 86. [PubMed: 10201120]
2. Chung C, Burdick JA. Engineering cartilage tissue. Advanced Drug Delivery Reviews 2008;60(2): 243–62. [PubMed: 17976858]
3. Hunziker EB. Articular cartilage repair: Basic science and clinical progress. A review of the current status and prospects. Osteoarthritis and Cartilage 2002;10(6):432–63. [PubMed: 12056848]
4. Farndale RW, Buttle DJ, Barrett AJ. Improved quantitation and discrimination of sulfated glycosaminoglycans by use of dimethylmethylene blue. Biochimica et Biophysica Acta 1986:883173–77.
5. Hollander AP, Heathfield TF, Webber C, Iwata Y, Bourne R, Rorabeck C, et al. Increased damage to type ii collagen in osteoarthritic articular cartilage detected by a new immunoassay. Journal of Clinical Investigation 1994;93(4):1722. [PubMed: 7512992]
6. Freed LE, Vunjak-Novakovic G. Cultivation of cell-polymer tissue constructs in simulated microgravity. Biotechnology and Bioengineering 1995;46(4):306–13. [PubMed: 18623317]
7. Brown MP, Trumble TN, Sandy JD, Merritt KA. A simplified method of determining synovial fluid chondroitin sulfate chain length. Osteoarthritis and Cartilage 2007;15(12):1443–45. [PubMed: 17632019]
8. Calabro A, Midura R, Wang A, West L, Plaas A, Hascall VC. Fluorophore-assisted carbohydrate electrophoresis (face) of glycosaminoglycans. Osteoarthritis and Cartilage 2001:916–22.
9. Riesle J, Hollander AP, Langer R, Freed LE, Vunjak-Novakovic G. Collagen in tissue-engineered cartilage: Types, structure, and crosslinks. Journal of Cellular Biochemistry 1998;71(3):313–27. [PubMed: 9831069]
10. Athanasiou KA, Agarwal A, Dzida FJ. Comparative study of the intrinsic mechanical properties of the human acetabular and femoral head cartilage. Journal of Orthopaedic Research 1994;12(3):340–49. [PubMed: 8207587]
11. Frank EH, Jin M, Loening AM, Levenston ME, Grodzinsky AJ. A versatile shear and compression apparatus for mechanical stimulation of tissue culture explants. Journal of Biomechanics 2000;33 (11):1523–27. [PubMed: 10940414]
12. Williamson AK, Chen AC, Sah RL. Compressive properties and function-composition relationships of developing bovine articular cartilage. Journal of Orthopaedic Research 2001;19(6):1113–21. [PubMed: 11781013]
13. Eggli PS, Hunzinker EB, Schenk RK. Quantitation of structural features characterizing weight- and less-weight-bearing regions in articular cartilage: A stereological analysis of medial femoral condyles in young adult rabbits. The Anatomical Record 1988;222(3):217–27. [PubMed: 3213972]
14. Ng L, Grodzinsky AJ, Patwari P, Sandy J, Plaas A, Ortiz C. Individual cartilage aggrecan macromolecules and their constituent glycosaminoglycans visualized via atomic force microscopy. Journal of Structural Biology 2003;143(3):242–57. [PubMed: 14572479]
15. Dean D, Han L, Grodzinsky AJ, Ortiz C. Compressive nanomechanics of opposing aggrecan macromolecules. Journal of Biomechanics 2006;39(14):2555–65. [PubMed: 16289077]
16. Bos KJ, Holmes DF, Kadler KE, McLeod D, Morris NP, Bishop PN. Axial structure of the heterotypic collagen fibrils of vitreous humour and cartilage. Journal of Molecular Biology 2001;306(5):1011–22. [PubMed: 11237615]
17. Wenger MPE, Bozec L, Horton MA, Mesquida P. Mechanical properties of collagen fibrils. Biophysical journal 2007;93(4):1255–63. [PubMed: 17526569]
18. Cowman MK, Li M, Balazs EA. Tapping mode atomic force microscopy of hyaluronan: Extended and intramolecularly interacting chains. 1998;75(4):2030–37.
19. Dudhia J. Aggrecan, aging and assembly in articular cartilage. Cellular and Molecular Life Sciences 2005;62(19):2241–56. [PubMed: 16143826]
20. Mauck RL, Yuan X, Tuan RS. Chondrogenic differentiation and functional maturation of bovine mesenchymal stem cells in long-term agarose culture. Osteoarthritis and Cartilage 2006;14(2):179–89. [PubMed: 16257243]

NIH-PA Author Manuscript

NIH-PA Author Manuscript

NIH-PA Author Manuscript

21. Im GI, Jung NH, Tae SK. Chondrogenic differentiation of mesenchymal stem cells isolated from patients in late adulthood: The optimal conditions of growth factors. Tissue engineering 2006;12(3): 527–36. [PubMed: 16579686]
22. Connelly JT, Wilson CG, Levenston ME. Characterization of proteoglycan production and processing by chondrocytes and bmscs in tissue engineered constructs. Osteoarthritis and cartilage 2008;16(9): 1092–100. [PubMed: 18294870]
23. Kopesky PW, Lee HY, Vanderploeg EJ, Kisiday JD, Frisbie DD, Ortiz C, et al. Adult equine bone-marrow stromal cells produce a cartilage-like ECM mechanically superior to animal-matched adult chondrocytes. Matrix Biology. 2010 in press.
24. Erickson IE, Huang AH, Chung C, Li RT, Burdick JA, Mauck RL. Differential maturation and structure-function relationships in mesenchymal stem cell- and chondrocyte-seeded hydrogels. Tissue Eng Part A 2009;15(5):1041–52. [PubMed: 19119920]
25. Scharstuhl A, Schewe B, Benz K, Gaissmaier C, Bühring HJ, Stoop R. Chondrogenic potential of human adult mesenchymal stem cells is independent of age or osteoarthritis etiology. Stem Cells 2007;25(12):3244–51. [PubMed: 17872501]
26. Nöth U, Steinert AF, Tuan RS. Technology insight: Adult mesenchymal stem cells for osteoarthritis therapy. Nat Clin Pract Rheumatol 2008;4(7):371–80. [PubMed: 18477997]
27. Roughley PJ, White RJ. Age-related changes in the structure of the proteoglycan subunits from human articular cartilage. J Biol Chem 1980;255(1):217–24. [PubMed: 7350154]
28. Sheiko SS, Moller M. Visualization of macromoleculesa first step to manipulation and controlled response. Chemical Reviews 2001;101(12):4099–124. [PubMed: 11740928]
29. Wilbur JL, Kumar A, Biebuyck HA, Kim E, Whitesides GM. Microcontact printing of self-assembled monolayers: Applications in microfabrication. Nanotechnology 1996;7(4):452–57.
30. Bhattacharjee S, Elimelech M. Surface element integration: A novel technique for evaluation of dlvo interaction between a particle and a flat plate. Journal of colloid and interface science 1997;193(2): 273–85. [PubMed: 9344528]
31. Patwari P, Kurz B, Sandy JD, Grodzinsky AJ. Mannosamine inhibits aggrecanase-mediated changes in the physical properties and biochemical composition of articular cartilage. Archives of Biochemistry and Biophysics 2000;374(1):79–85. [PubMed: 10640399]
32. Nagase H, Kashiwagi M. Aggrecanases and cartilage matrix degradation. Arthritis Res Ther 2003;5 (2):94–103. [PubMed: 12718749]
33. Oshita H, Sandy JD, Kiichi Suzuki, Akaike A, Bai Y, Sasaki T, et al. Mature bovine articular cartilage contains abundant aggrecan that is c-terminally truncated at ala719-ala720, a site which is readily cleaved by m-calpain. Biochem J 2004:382253–59.
34. Kopesky PW, Vanderploeg EJ, Sandy JD, Kurz B, Grodzinsky AJ. Self-assembling peptide hydrogels modulate in vitro chondrogenesis of bovine bone marrow stromal cells. Tissue Engineering Part A 2009;16(2):465–77. [PubMed: 19705959]
35. Deutsch AJ, Midura RJ, Plaas AHK. Structure of chondroitin sulfate on aggrecan isolated from bovine tibial and costochondral growth plates. Journal of Orthopaedic Research 1995;13(2):230–39. [PubMed: 7722760]
36. Brown MP, West LA, Merritt KA, Plaas AHK. Changes in sulfation patterns of chondroitin sulfate in equine articular cartilage and synovial fluid in response to aging and osteoarthritis. American Journal of Veterinary Research 1998:59786–91.
37. Sandy JD, Verscharen C. Analysis of aggrecan in human knee cartilage and synovial fluid indicates that aggrecanase (adamts) activity is responsible for the catabolic turnover and loss of whole aggrecan whereas other protease activity is required for c-terminal processing in vivo. Biochemical Journal 2001;358(Pt 3):615. [PubMed: 11535123]
38. Qureshi HY, Ahmad R, Sylvester J, Zafarullah M. Requirement of phosphatidylinositol 3-kinase/akt signaling pathway for regulation of tissue inhibitor of metalloproteinases-3 gene expression by TGF-β in human chondrocytes. Cellular Signalling 2007;19(8):1643–51. [PubMed: 17376651]
39. Moulharat N, Lesur C, Thomas M, Rolland-Valognes G, Pastoureau P, Anract P, et al. Effects of transforming growth factor-[beta] on aggrecanase production and proteoglycan degradation by human chondrocytes in vitro. Osteoarthritis and Cartilage 2004;12(4):296–305. [PubMed: 15023381]

NIH-PA Author Manuscript

NIH-PA Author Manuscript

NIH-PA Author Manuscript

40. Inerot S, Heinegård D, Audell L, Olsson SE. Articular-cartilage proteoglycans in aging and osteoarthritis. Biochemical Journal 1978;169(1):143. [PubMed: 629741]
41. Thonar EJ, Buckwalter JA, Kuettner KE. Maturation-related differences in the structure and composition of proteoglycans synthesized by chondrocytes from bovine articular cartilage. Journal of Biological Chemistry 1986;261(5):2467–74. [PubMed: 3080435]
42. Plaas AHK, Wong-Palms S, Roughley PJ, Midura RJ, Hascall VC. Chemical and immunological assay of the nonreducing terminal residues of chondroitin sulfate from human aggrecan. J Biol Chem 1997;272(33):20603–10. [PubMed: 9252375]
43. Brown MP, Trumble TN, Plaas AHK, Sandy JD, Romano M, Hernandez J, et al. Exercise and injury increase chondroitin sulfate chain length and decrease hyaluronan chain length in synovial fluid. Osteoarthritis and Cartilage 2007;15(11):1318–25. [PubMed: 17543547]
44. Carney SL, Billingham MEJ, Muir H, Sandy JD. Structure of newly synthesised (^{35}s)-proteoglycans and (^{35}s)-proteoglycan turnover products of cartilage explant cultures from dogs with experimental osteoarthritis. Journal of Orthopaedic Research 1985;3(2):140–47. [PubMed: 3998892]
45. Midura RJ, Calabro A, Yanagishita M, Hascall VC. Nonreducing end structures of chondroitin sulfate chains on aggrecan isolated from swarm rat chondrosarcoma cultures. Journal of Biological Chemistry 1995;270(14):8009. [PubMed: 7713901]
46. Hascall VC, Midura RJ, Sorrell JM, Plaas AH. Immunology of chondroitin/dermatan sulfate. Advances in experimental medicine and biology 1995:376205.
47. Maroudas A, Muir H, Wingham J. The correlation of fixed negative charge with glycosaminoglycan content of human articular cartilage. Biochimica et biophysica acta 1969;177(3):492. [PubMed: 4239606]
48. Buschmann MD, Grodzinsky AJ. A molecular model of proteoglycan-associated electrostatic forces in cartilage mechanics. J Biomech Eng 1995;117(2):179–92. [PubMed: 7666655]
49. Lee HY, Han L, Daher L, Bonaparte R, Roughley PJ, Ortiz C, et al. Age-related changes in human aggrecan molecular structure and its nanomechanical properties. Trans 54rd Orthop Res Soc, San Francisco. 2008

NIH-PA Author Manuscript

NIH-PA Author Manuscript

NIH-PA Author Manuscript

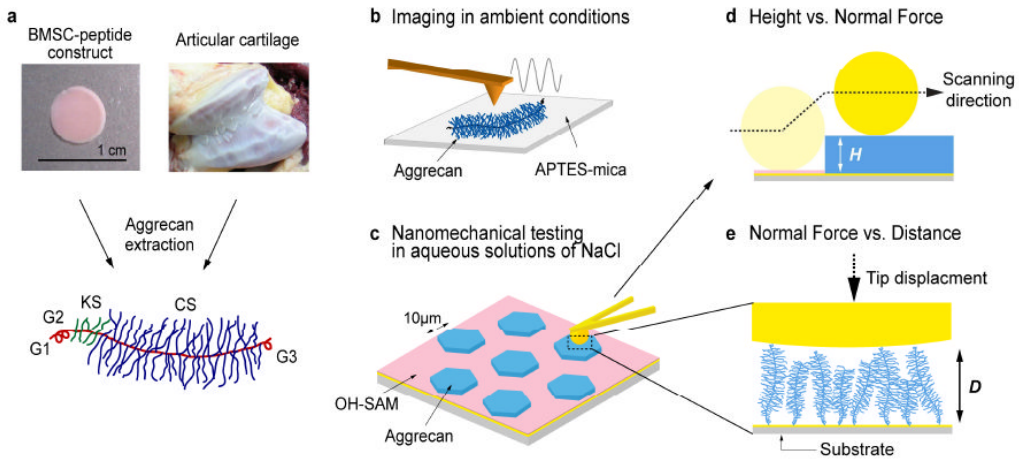

Fig 1.

(a). Aggrecan was extracted from adult equine BMSC-peptide gels (after 21 days of culture) and from adult equine articular cartilage. The model of full-length aggrecan shows the globular domain structures labelled as G1,G2,G3, linked by a core protein substituted with keratan sulfate (KS) and, chondroitin sulfate (CS). (b) An illustration of aggrecan imaging using AFM tapping mode. Aggrecan molecules were immobilized on the APTES-modified mica substrate in a flattened conformation and imaged by a sharp silicon probe tip. (c) Illustrations of AFM nanomechanical testing. Micro-contact-printed aggrecan patterns were surrounded by self-assembled monolayer molecules (11-mercaptoundecanol, $HS(CH_2)_{11}OH$, OH-SAM). A spherical gold-coated glass tip (functionalized with of OH-SAM) was used to scan and compress the aggrecan patterns. The experiment was performed in 0.001-1.0M NaCl (pH ~ 5.6). (d) Height-normal force measurement: contact mode imaging was used to apply a range of normal compressive forces while scanning across the patterned surface to measure the compressed height *H* of aggrecan. (e) Normal force-distance measurements: direct compression of aggrecan was performed by having the probe tip approach the surface perpendicular to the plane of the substrate and measuring the force as a function of tip-to-substrate distance *D*.

NIH-PA Author Manuscript
NIH-PA Author Manuscript
NIH-PA Author Manuscript

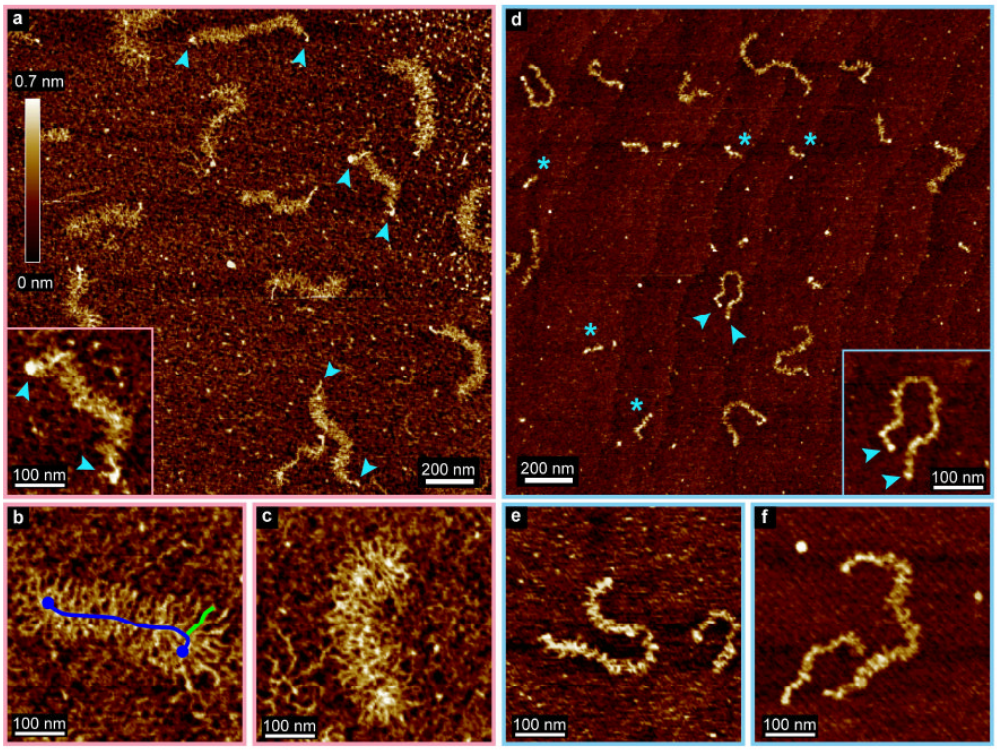

Fig. 2.

AFM height images of aggrecan monomers. (a)-(c) Aggrecan produced by adult equine BMSCs seeded in peptide hydrogel. (d)-(f) Aggrecan extracted from adult equine articular cartilage. In (a) and (d), the globular domains of full length aggrecan are indicated by arrows. Example of short degraded aggrecan fragments (~100 nm) are marked by asterisks in (d). Examples of core protein and GAG chain traces are shown in (b).

NIH-PA Author Manuscript

NIH-PA Author Manuscript

NIH-PA Author Manuscript

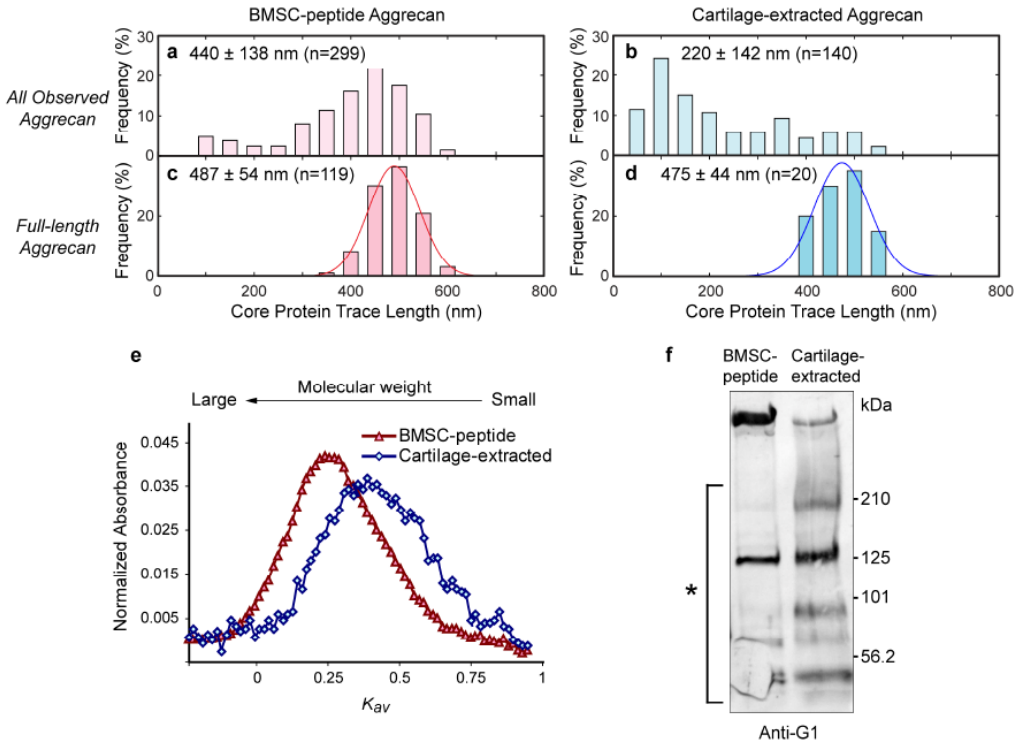

Fig. 3.

Core protein analyses. Core protein trace length distributions of (a) BMSC-peptide aggrecan and (b) cartilage-extracted aggrecan measured from the AFM height images. (Mean ± SD is noted in each histogram. *n* = number of measured aggrecan molecules.) The distributions of the two core protein populations (a,b) are markedly different (K-S test, $p<0.0001$). Core protein trace length distributions of *full-length* (c) BMSC-peptide aggrecan and (d) cartilage-extracted aggrecan. Gaussian curves were fit to both distributions; the goodness of fit R^2 is 0.997 and 0.974 in (c) and (d), respectively. These two core protein length distributions (c,d) are not significantly different (two-tailed t test, $p = 0.3531$.) (e) Elution profiles of BMSC-peptide and cartilage-extracted aggrecan on a Sephacryl S-1000 column. $K_{av} = 0.25$ for the BMSC-peptide aggrecan and 0.42 for the cartilage-extracted aggrecan, indicating the greater hydrodynamic size of BMSC-peptide aggrecan. (f) Western blot analysis with anti-G1 antibody. High molecular weight core protein as well as low molecular weight core fragment species (*) were detected in both BMSC-peptide and cartilage-extracted aggrecan samples.

NIH-PA Author Manuscript

NIH-PA Author Manuscript

NIH-PA Author Manuscript

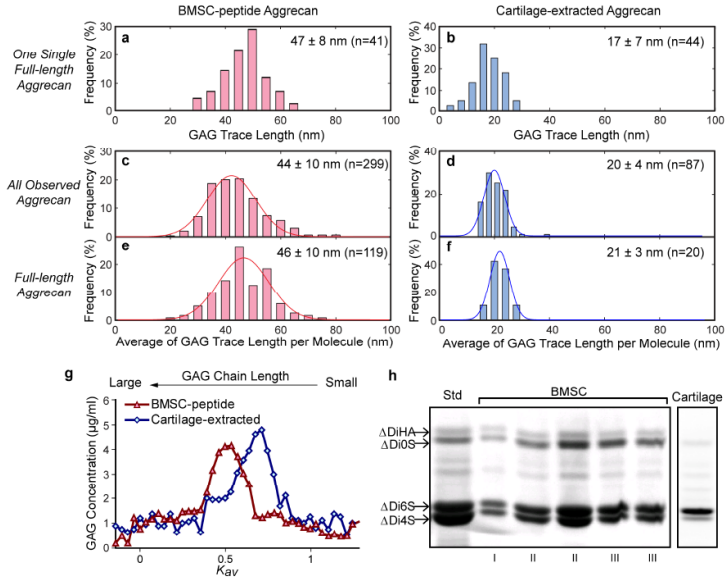

Figure 4.

GAG chain length and composition analysis. Distribution of GAG trace lengths on one selected *single* representative (a) BMSC-peptide aggrecan and (b) cartilage-extracted *full-length* aggrecan. Mean ± SD is noted in each histogram. *n* = number of measured GAG chains. Distribution of average GAG chain lengths for multiple (c) BMSC-peptide aggrecan and (d) cartilage-extracted aggrecan. *n* = number of measured aggrecan molecules. Distribution of average GAG chain length on multiple *full-length* (e) BMSC-peptide aggrecan and (f) cartilage-extracted aggrecan. *n* = number of measured aggrecan molecules. The goodness of the Gaussian fit R^2 in (c)-(f) is 0.971, 0.968, 0.901 and 0.999, respectively. (g) Superose 6 chromatography shows the BMSC-peptide GAG population is longer than the cartilage-extracted GAG population with K_{av} =0.50 and 0.71, respectively. (h) FACE analysis of aggrecan produced by BMSCs derived from 3 adult horses and that of aggrecan extracted from adult cartilage. The BMSC-peptide aggrecan showed an approximately equal amount of ΔDi6S and ΔDi4S in contract to the increased ΔDi6S content of cartilage-extracted aggrecan.

NIH-PA Author Manuscript

NIH-PA Author Manuscript

NIH-PA Author Manuscript

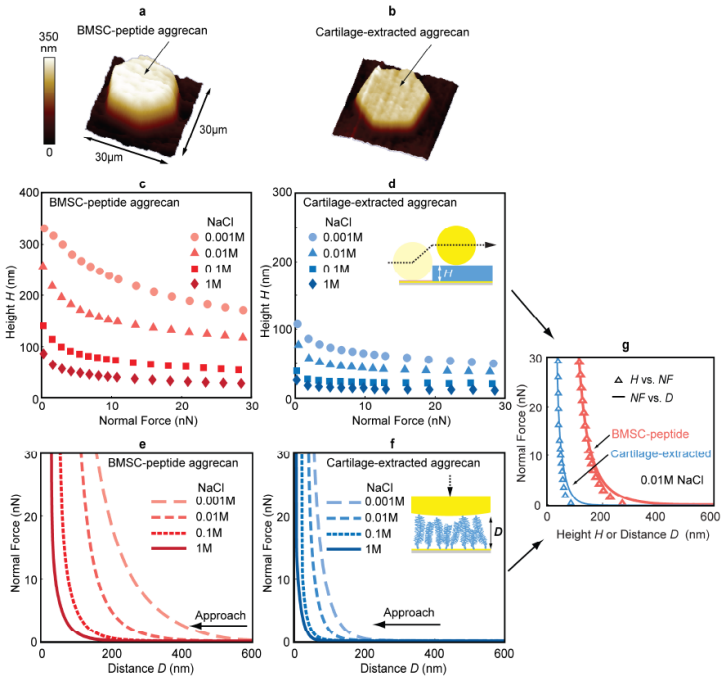

Fig. 5.

Nanomechanical testing. (a,b) AFM three-dimensional height images of (a) BMSC-peptide and (b) cartilage-extracted aggrecan chemically end-grafted on gold substrates and patterned by micro-contact printing. The images were taken in 0.001M NaCl with a minimal applied normal force ~100 pN. (c,d) Compressed aggrecan height *H* versus normal force curves of (c) BMSC-peptide and (d) cartilage-extracted aggrecan in different ionic strength aqueous solution were measured by contact mode AFM. Insert in (d) shows the direction of the scan and the corresponding compressed height *H*. Each data point represents the average aggrecan height from 8 scans across the pattern at a given normal force and NaCl concentration. The standard deviation (SD) of each data point is smaller than the size of the data point. (e,f) Normal force versus distance curves of (e) BMSC-peptide and (f) cartilage-extracted aggrecan during normal compression as shown in the insert in (f). The probe tip approaches the substrate perpendicular to the plane of the substrate. Each curve is an average of 30 approaches in different locations on the pattern. The SD of each averaged curve is smaller than the line width. (g) Comparison of the height-normal force measurement (open triangles, replotted from Fig. 5c,d, 0.01M NaCl) and normal force-distance measurements (lines, replotted from Fig. 5e,f, 0.01M NaCl). Data measured using two different methods well coincide. Some slight discrepancy at low normal force (< 5 nN) is possibly due to the finite normal force necessary for maintaining stable feedback during the contact mode scanning.

NIH-PA Author Manuscript

NIH-PA Author Manuscript

NIH-PA Author Manuscript

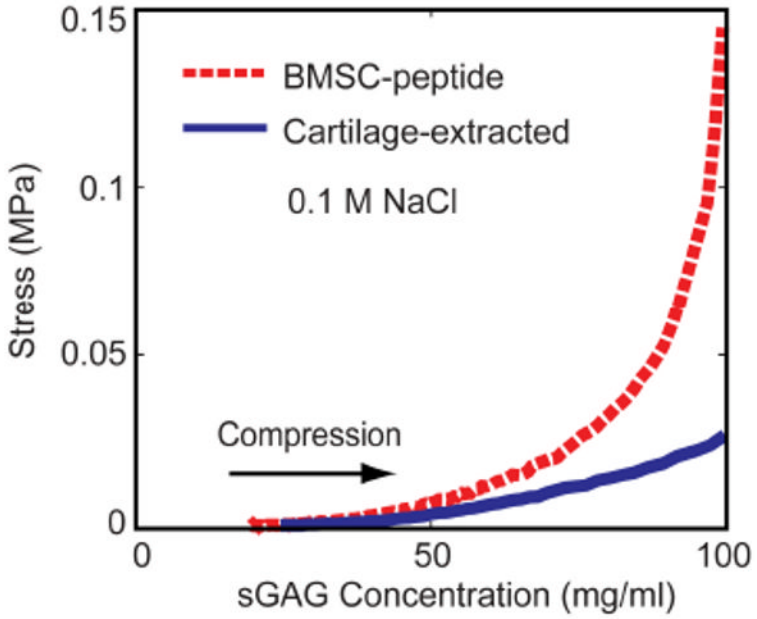

Fig. 6.

Stress-sGAG concentration curves converted from the force-distance curves in Fig 5 e,f (0.1M NaCl). The initial uncompressed sGAG concentration was the total sGAG amount measured by DMMB divided by the aggrecan pattern volume measured by AFM height images. Normal stress was calculated from the force using the surface element integration method[30]. Upon compression by the probe tip, the sGAG density of the end-grafted aggrecan under the probe tip increased due to the decrease in compressed volume. When both aggrecan patterns were compressed to the same sGAG concentration, BMSC-peptide aggrecan exhibited greater stress than the cartilage-extracted aggrecan. (note: GAG concentration in native tissue is 20-80 mg/ml)[47]. Each curve is an average of 30 approaches in different locations on the aggrecan pattern. The 95% confidence intervals of each averaged curve are smaller than the line width.